Water Quality and Sediment Behaviour of the Future: Predictions for the 21st Century (Proceedings of Symposium HS2005 at IUGG2007, Perugia, July 2007). IAHS Publ. 314, 2007.

Modelling discharge, water chemistry and sediment load from a subarctic river basin: the Tanana River, Alaska

KAZUHISA A. CHIKITA[1], TOMOYUKI WADA[1], ISAO KUDO[2], DAISAKU KIDO[1], YU-ICHI NARITA[1] & YONGWON KIM[3]

1 *Laboratory of Physical Hydrology, Faculty of Science, Hokkaido University, Sapporo 060-0810, Japan*
chikita@mail.sci.hokudai.ac.jp

2 *Faculty of Fisheries Sciences, Hokkaido University, Hakodate 041-8611, Japan*

3 *International Arctic Research Center, the University of Alaska, Fairbanks, Alaska 99775-7340, USA*

Abstract With reference to elevation effects on air temperature and rainfall, the time series of discharge, suspended sediment concentration (SSC) and SiO_2 in the Tanana River, Alaska, are simulated by a conceptual model, the tank model. The simulations are reasonable (correlation coefficient r = 0.684 to 0.953) for all the time series obtained in the glacier-melt periods of 2002, 2004 and 2005. The smog from large forest fires in the summers of 2004 and 2005 sporadically covered the glacierized regions in the river basin, which were defined by field observation and using satellite imagery. The correlation for the discharge series was relatively low in or around the smog-covered periods. This is caused by the overestimation of calculated glacier-melt discharge. The runoff analyses revealed that, in spite of the 5.6% glacierized area, the glacier-melt discharge comprises 35.2 to 54.2% of the river discharge. The simulations of the SSC and SiO_2 series suggest that the suspended sediment originates mostly from glacierized regions, and SiO_2 mainly from the mineral layer in the permafrost regions.

Key words forest fires; glacier; permafrost; sediment load; Tanana River; tank model

INTRODUCTION

The drainage basins of subarctic to arctic large rivers such as the Yukon River, Alaska, and MacKenzie River, Canada, are composed of extensive permafrost regions and glacierized mountainous regions. The river runoff in summer can occur through runoff generated by rainfall in the permafrost regions and glacier-melt discharge in the glacierized regions (Brabets *et al.*, 2000). The permafrost in the Yukon River basin occurs discontinuously in the needleleaf (dominantly, spruce) forests and extensively in the alluvial deposits around the river channels (Ferrians, 1965; Brown *et al*., 1997). Large forest fires occurred in the permafrost regions in the summers of 2004 and 2005 (Division of Forestry, Alaska Department of Natural Resources: URL http://www.dnr.state.ak.us/forestry/). The smog from forest fires sporadically covered glacierized regions, which could change the heat and water balances of the glaciers by decreasing the solar radiation input. The Tanana River, a tributary of the Yukon River, has glacierized regions in the headwater Alaska Range and Wrangell Mountains, thus its discharge is likely sensitive to be sensitive to glacier-melt.

In this study, time series of discharge, suspended sediment concentration (SSC) and SiO_2 in the Tanana River, Alaska, are simulated by a conceptual model, the tank model (Sugawara, 1972; Sugawara *et al*., 1983). This model allows the contribution of glacier-melt and rainfall to the Tanana River discharge to be quantitatively estimated, and, in turn, a discussion of sediment and SiO_2 sources. A change in the heat and water balances of glaciers due to the smog cover is inferred by using hydrological and meteorological data and by comparing calculations with observations for discharge and SSC time series.

STUDY AREA AND METHODS

The Tanana River, Alaska, is located in the subarctic area south of the Arctic Circle (66°33′N). It is 621 km long, and is occupied by extensively distributed permafrost regions and glacierized regions concentrated in the Alaska Range and Wrangell Mountains (Fig. 1). Site NEN (64°33′N, 149°5′W; No. 1 in Fig. 1) is a US Geological Survey (USGS) gauging station for river stage, 208 km upstream of the confluence to the Yukon River. The drainage area upstream of site NEN is 6.63×10^4 km^2.

Water turbidity and temperature of the Tanana River were monitored at 1 hourly intervals at site NEN in the summers of 2002, 2004 and 2005, by using a self-recording turbidimeter of infrared-ray back scattering type and a temperature data logger, respectively (Chikita *et al*., 2006; Kido *et al*., 2007). The 10-sample averaged turbidity values were converted to suspended sediment concentrations (SSC) (mg L^{-1}), using the relationship ($r^2 = 0.994$) between turbidity and simultaneous measurements of SSC obtained from the filtration of river water. Hourly discharge data at site NEN were supplied by the USGS, Fairbanks. The suspended sediment load, L (kg s^{-1}), was calculated by $L = C \times Q$, where C is the SSC (g L^{-1}) and Q is the discharge (m^3 s^{-1}). Burrows *et al.* (1981) pointed out that, in the Tanana River, the suspended load and washload are significantly larger than the bedload. The SiO_2 concentration was measured by colorimetry (QuAATro, Bran Luebbe, Inc.) for river water sampled once every 4 to 20 days at site NEN in 2005.

There are 15 weather stations operated by USGS, NOAA (National Oceanic and Atmospheric Administration) and WRCC (Western Regional Climate Center) upstream of site NEN (Fig. 1). Hourly air temperature and rainfall data were supplied from these agencies. Using the data sets at the weather stations, the spatial distribution of daily mean air temperature over the drainage basin upstream of site NEN was determined on the basis of the Thiessen method, by which the drainage basin was partitioned into 15 sub-areas (Fig. 2). The air temperature within each of the 15 sub-areas was corrected for elevation by applying the lapse rate of 0.6°C per 100 m to the National Elevation Dataset (NED) (http://seamless.usgs.gov/) of the river basin (March, 2000). By superimposing a Landsat image of 2001 on the NED, the glacierized area was determined as 5.6% of the drainage area. The glacierized regions are located in the Alaska Range (within sub-areas 1, 7–10 and the northern part of 11) and in the Wrangell Mountains (within sub-areas 14 and 15 and the southern part of 11) (Fig. 2). The smog-covered periods for glacierized regions were identified using daily visibility data at Paxson (No. 8 in Fig. 1) and MODIS images, which were taken by the

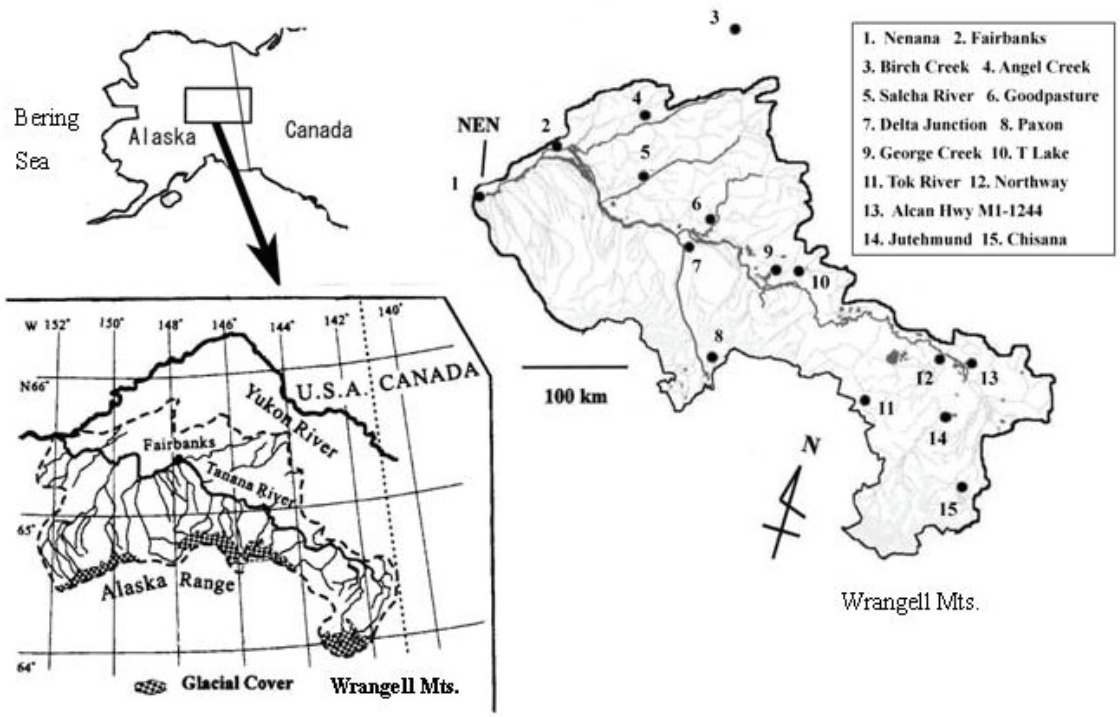

Fig. 1 Drainage basin of the Tanana River (dotted line on the left) and observation sites in the Tanana River basin upstream of site NEN (modified after Brabets *et al*., 2000). The 15 weather stations are numbered upstream of site NEN, a USGS gauging station.

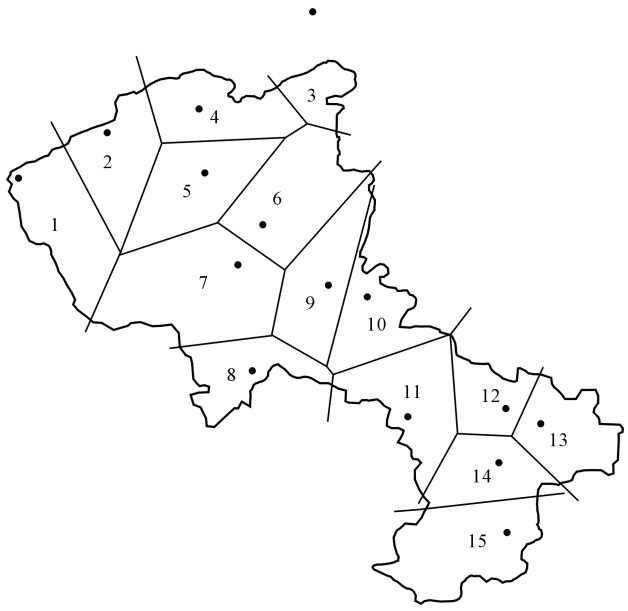

Fig. 2 Sub-areas separated by the location of the 15 weather stations upstream of site NEN (Fig. 1) based on the Thiessen method (Chikita *et al*., 2006).

Terra satellite and were available from the Geographic Information Network of Alaska (GINA) at the University of Alaska.

An elevation effect on the rainfall in each sub-area was taken into account by downloading from http://www.climatesource.com/ elevation-corrected monthly rainfall

data for June averaged over 1961 to 1990 in the whole Alaska, and assuming the elevation effect to be identical to that of the rainfall during the observation periods of 2002, 2004 and 2005. As a result, the corrected rainfalls were ~30% larger than the original values.

OBSERVATIONAL RESULTS AND DISCUSSION

Hydrological, thermal and meteorological conditions

Figure 3 shows temporal variations of discharge, sediment load, suspended sediment concentration (SSC), water temperature, daily mean air temperature (T_{NEN}) at site NEN, the daily rainfall averaged upstream of site NEN, and the daily mean air temperature (T_{gl}) over the glacierized regions in June to September of 2004 and 2005. SSC recording failed twice in July and August 2004, and zero turbidity was recorded probably due to the probe being obscured by suspended organic matter such as leaves or roots. The temporal pattern of the sediment load is very similar to that of SSC, which suggests it is influenced more by concentration than discharge. The glacier-melt in 2004 was probably larger than in 2005, since the air temperature in the glacierized

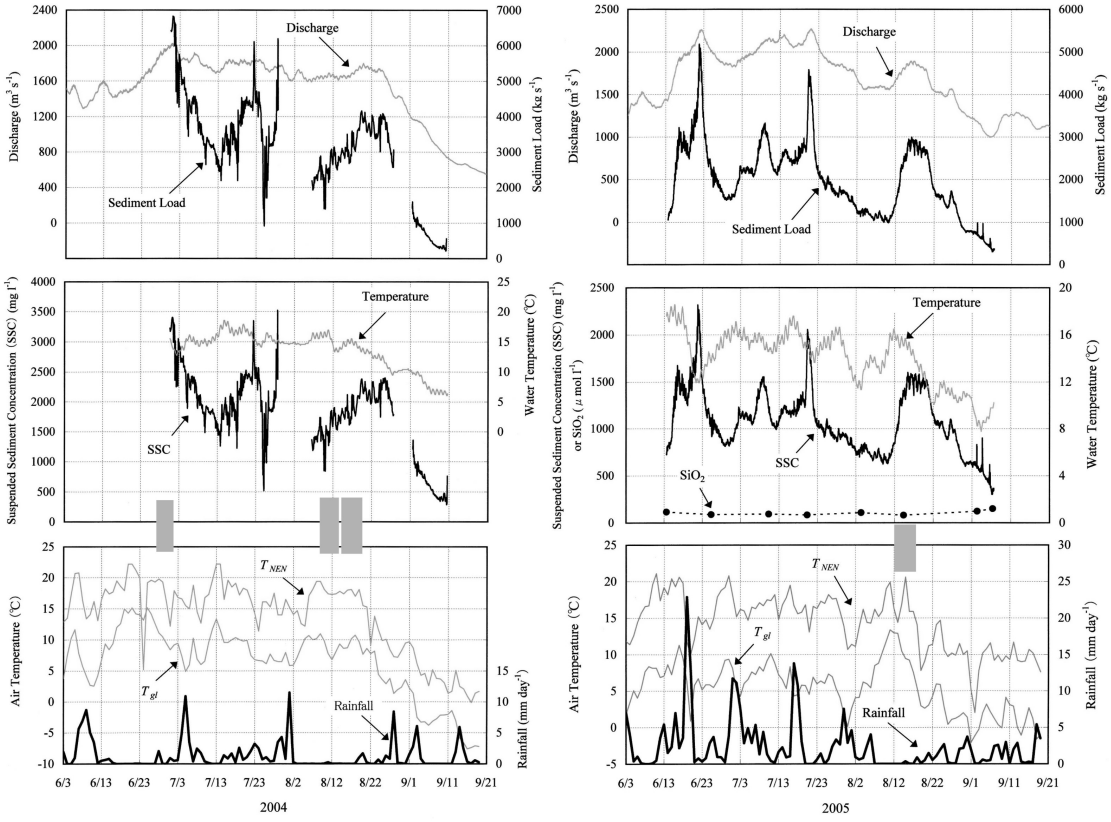

Fig. 3 Temporal variations of discharge, sediment load, suspended sediment concentration (SSC), water temperature and SiO_2 at site NEN in the glacier-melt seasons of 2004 and 2005. T_{NEN} and T_{gl} indicate the daily mean air temperature at site NEN and in the whole glacierized regions, respectively. The daily rainfall is averaged for the drainage basin upstream of site NEN. The three grey bands correspond to the smog-covered periods.

regions (T_{gl}) in June to August 2004 was consistently higher than in 2005, except for mid-August. The relatively high SSC and sediment load in 2004 therefore likely results from the relatively large sediment supply from glacierized regions. The large rainfalls in June and July 2005 sporadically induced short-term sediment runoff in the Tanana River. Water temperature decreased whenever SSC increased. This suggests that the suspended sediment amount in water depends on the magnitude of glacier-melt or rainfall runoff on cool days. The discharge, sediment load and thermal flux at site NEN are thus highly sensitive to rainfall over the drainage basin and air temperature over the glacierized regions. The SiO_2 time series for 2005 indicates that SiO_2 decreases with increasing river discharge. This suggests a supply of SiO_2 in base flow from the permafrost regions.

The smog from large forest fires in 2004 and 2005 covered the glacierized regions for the four periods of 26 June to 1 July, 10–13 August, 15–19 August 2004, and 12–17 August 2005 (grey bands in Fig. 3). A decrease in air temperature in glacierized regions occurred on rainy days, but was not found during the smog-covered periods. A decrease in the glacier-melt amount during the smog-covered periods could thus be induced only by decreased solar radiation.

MODELLING

In order to clarify the contribution of glacier-melt and rainfall to the discharge and sediment load at site NEN, and to identify sediment and SiO_2 sources, the simulation of discharge, SSC and SiO_2 time series in Fig. 3 was undertaken using a tank model. The tank model, a conceptual model, has been used for river runoff analyses (Sugawara, 1972; Motoyama *et al*., 1983; Mizunuma & Chiu, 1985; Yue & Hashino, 2000; Chikita *et al*., 2006) and for sediment runoff analyses (Osawa & Sakai, 2002; Kido *et al*., 2007). Water chemistry time series have also been simulated by the tank model (Kato *et al*., 2003). Considering the characteristics of discharge (Woo & Marsh, 2005; Kido *et al*., 2007), one tank (a glacial tank) and three serial tanks (permafrost tanks) were applied in simulating the glacierized and permafrost regions, respectively.

Glacier-melt amount, evapotranspiration and rainfall

The glacier-melt amount in glacierized regions and the evapotranspiration in permafrost regions were evaluated as water input into the glacial tank and water output from the top of permafrost tanks, respectively. Rainfall onto the glacierized and permafrost regions was considered as water input to the glacial tank and the top of permafrost tanks.

The total glacier-melt amount was calculated by using the spatial distribution of daily mean air temperature corrected for elevation over the glacierized regions, and by the following positive degree-day approach (PDDA) (Braithwaite, 1995):

$$M = T_a \times f \tag{1}$$

where M is the glacier-melt amount (mm day^{-1}) and f is the degree day factor (mm day^{-1} °C^{-1}). The values of f = 3.5 to 5.0 for the snow cover and f = 7.0 to 10.0 for the ice

cover were obtained by March (2000) in the Gulkana Glacier, Alaska. Based on the results of Kido *et al*. (2007) for the Gulkana Glacier, $f = 3.5$ and $f = 7.0$ were adopted for the snow and ice surfaces, respectively. Sublimation and meltwater evaporation from the glacierized regions were neglected.

Using the elevation-corrected air temperature, the daily potential evapotranspiration, PET (mm day^{-1}), in the permafrost regions was calculated by the following equation (Hamon, 1963; Dingman, 2002):

$$PET = 29.8 \cdot D \cdot \frac{e_s(T_a)}{T_a + 273.2} \tag{2}$$

where PET is the daily potential evapotranspiration (mm day^{-1}), D is the potential day length and e_s is the saturation vapour pressure (kPa) at the daily mean temperature, T_a (°C). The potential day length, D, was calculated by using the declination of the sun, the latitude and the angular velocity of the Earth's rotation (Dingman, 2002). The PET in equation (2) was summed as PET_{sum} over each observation period of 2002, 2004 and 2005, and the total actual evapotranspiration, ET_{sum}, was evaluated by Pike's equation (Dingman, 2002):

$$ET_{sum}{}^{i} = W_i / \left[1 + (W_i / PET_{sum}{}^{i})^2\right]^{1/2} \tag{3}$$

where $ET_{sum}{}^{i}$ and $PET_{sum}{}^{i}$ are the total actual and potential evapotranspiration in the ith sub-area (i = 1 to 15) in Fig. 2, respectively, and W_i is the total rainfall for the observation period in the ith sub-area. The evapotranspiration ratio, $\alpha_i = ET_{sum}{}^{i} / PET_{sum}{}^{i}$, for each sub-area was obtained for each observation period, and the daily actual evapotranspiration in each sub-area was calculated by multiplying PET in equation (1) by α_i on the assumption that α_i is constant over each observation period.

The structure and parameters of tanks

Considering the damping of flood waves during their downstream propagation, the drainage basin upstream of site NEN was partitioned into three sections: Section 1 comprising sub-areas No. 1 to5; Section 2 comprising sub-areas No. 6 to 10; and Section 3 comprising sub-areas No. 11 to 15 (Figs 2 and 4). The structure of tanks in relation to these sections is shown in Fig. 5. The tank in Series No. 2 and No. 4 corresponds to the glacial tank and the three serial tanks in Series No. 1, No. 3 and No. 5 to the permafrost tanks. The glacial tank is assigned to Section 2 and Section 3 containing the glacierized regions. The top, middle and bottom tanks for the permafrost regions correspond to surface runoff, intermediate runoff and base flow, respectively. The base flow includes the ice-melt discharge from the active layer and the groundwater discharge from non-permafrost areas, since the permafrost is discontinuously distributed. The tank parameters, α_{ij}, β_{ij}, d_{ij} and h_{ij} (i = 1 to 5, j = 1 to 4) were arbitrarily determined to give the best fit to the hydrograph obtained in 2002. The lag time of the tank series to discharge at site NEN was assumed to be constant.

For the analysis of sediment runoff, a sediment rating curve was applied only to the discharge from each glacial tank on the assumption that the dominant sediment

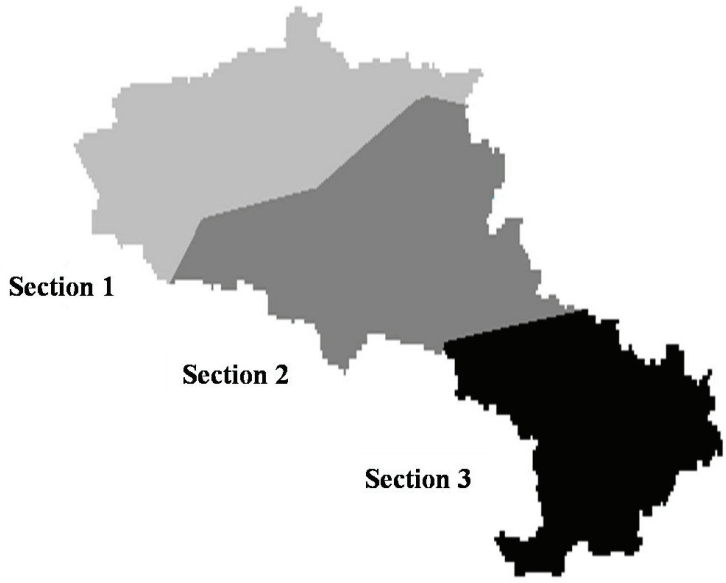

Fig. 4 Tanana River basin separated into three sections, according to the sub-areas depicted in Fig. 2.

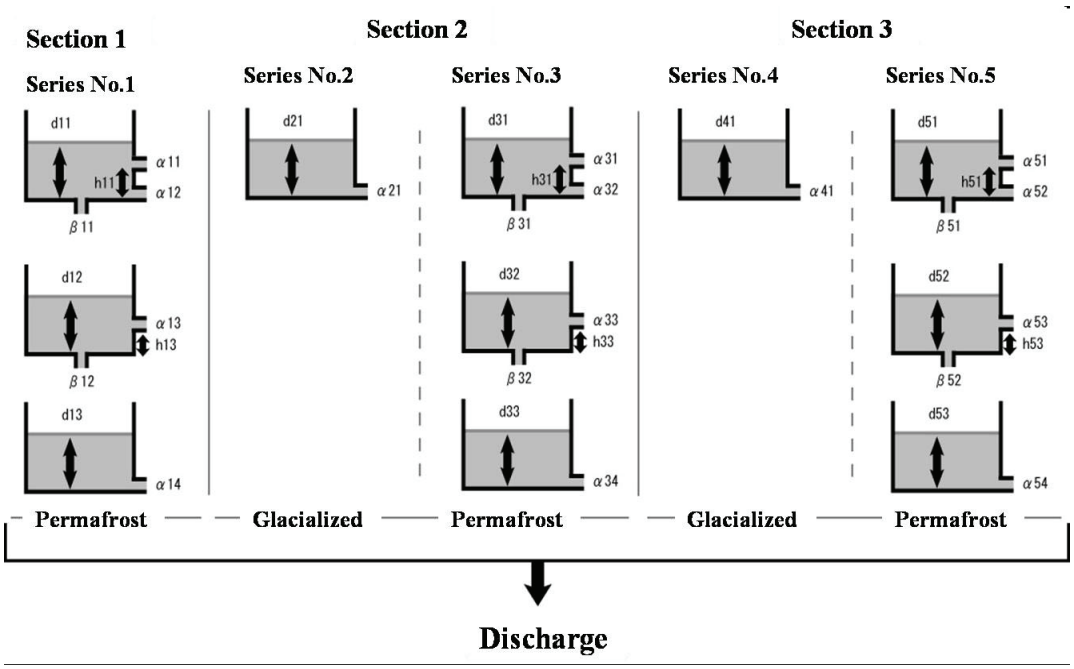

Fig. 5 Tanks assigned to the three sections of the Tanana River basin (Fig. 4).

supply is from the glacierized regions. The sediment rating curve is expressed by $L = aq^{b}$, where L is the sediment yield per unit area per unit time (kg m^{-2} s^{-1}), q is the specific discharge (mm s^{-1}) from the glacial tank, and a and b are the empirical coefficients. The two coefficients, a and b, were determined to give the best fit to the observed suspended sediment concentration series. The deposition and re-suspension of suspended sediment during the transport in the river channels were neglected. For

the analysis of the SiO_2 time series, a constant SiO_2 concentration was assigned to

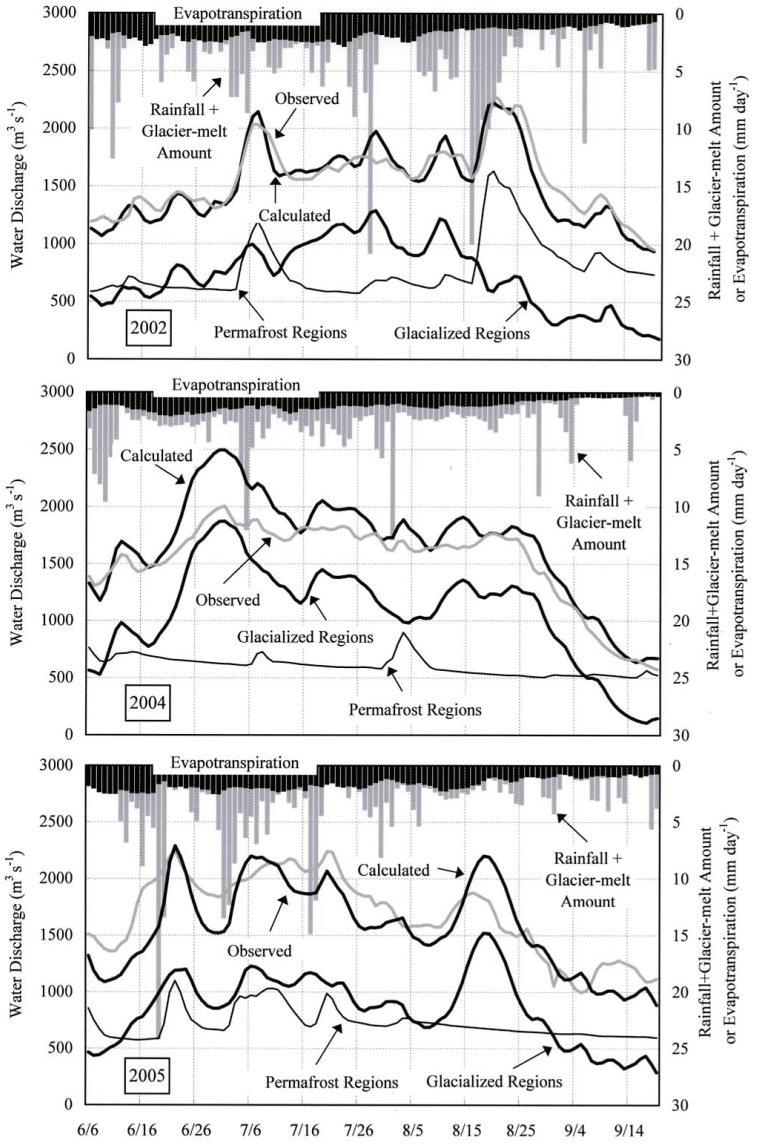

Fig. 6 Comparison between observed and simulated hydrographs. The calculated discharge is divided into that originating from the permafrost regions and that from the glacierized regions. The total input to the drainage basin by rainfall and glacier-melt, and the output from the permafrost regions by evapotranspiration, are also shown.

discharge from the bottom permafrost tank corresponding to base flow, and the equation, $L_{SI} = cq^d$, where L_{SI} is the SiO_2 amount per unit area per unit time (μmol m^{-2} s^{-1}) and c and d are constants, was applied to discharge from the glacial tank.

Simulation results

Simulated hydrographs and their comparison with the observed hydrographs are shown for 2002, 2004 and 2005 in Fig. 6. The tank parameters, α_{ij}, β_{ij}, d_{ij} and h_{ij} (i = 1 to 5, j = 1 to 4), are listed in Table 1. Lag times to the discharge at site NEN of the tank series

No. 1 to No.5 were held constant at 1, 4, 2, 5 and 3 days, respectively. The simulated

Table 1 Tank parameters used for the simulation of flow hydrographs at site NEN.

Section 1	α_{11} (h^{-1})	α_{12} (h^{-1})	α_{13} (h^{-1})	α_{14} (h^{-1})	β_{11} (h^{-1})	β_{12} (h^{-1})
	2.6×10^{-3}	3.6×10^{-4}	4.8×10^{-3}	7.6×10^{-4}	2.5×10^{-3}	6.6×10^{-3}
	h_{11} (mm)	h_{13} (mm)	d_{11} (mm)	d_{12} (mm)	d_{13} (mm)	
	14	6.8	0.6	10	21	
Section 2	α_{21} (h^{-1})	d_{21} (mm)	α_{31} (h^{-1})	α_{32} (h^{-1})	α_{33} (h^{-1})	α_{34} (h^{-1})
	$1.\ 6\times10^{-2}$	50	8.2×10^{-4}	0	2.7×10^{-4}	1.7×10^{-3}
β_{31} (h^{-1})	β_{32} (h^{-1})	h_{31} (mm)	h_{33}(mm)	d_{31} (mm)	d_{32} (mm)	d_{33} (mm)
6.4×10^{-3}	1.6×10^{-4}	8.0	0	0.6	10	21
Section 3	α_{41} (h^{-1})	d_{41} (mm)	α_{51} (h^{-1})	α_{52} (h^{-1})	α_{53} (h^{-1})	α_{54} (h^{-1})
	5.4×10^{-3}	100	8.9×10^{-4}	0	3.4×10^{-4}	1.1×10^{-3}
β_{51} (h^{-1})	β_{52} (h^{-1})	h_{51} (mm)	h_{53} (mm)	d_{51} (mm)	d_{52} (mm)	d_{53} (mm)
5.6×10^{-3}	6.2×10^{-4}	8.2	0	0.5	10	21

hydrograph was separated into the discharge from the glacierized and permafrost regions. For comparison, the daily rainfall plus daily glacier-melt amount in the glacierized regions and the evapotranspiration from the permafrost regions are also shown in Fig. 6. The correlation between the observed and calculated discharge is very significant at r = 0.951, 0.953 and 0.882 for 2002, 2004 and 2005, respectively, irrespective of the constant tank parameters (Table 1). This suggests that runoff pathways of the glacierized and permafrost regions do not change greatly from year to year. The discharge from the glacierized regions is larger than that from the permafrost regions until mid-August to early September, but thereafter, with decreasing air temperature, it is smaller. The contribution of the discharge at site NEN from the glacierized regions is simulated as 47.0% in 2002, 61.3% in 2004 and 52.2% in 2005, while that from glacial melt alone was simulated as 35.2 % in 2002, 54.2% in 2004 and 42.0% in 2005. The Tanana River could thus be "glacial", though the glacierized area is only ~5.6% of the total drainage area. Most of rainfall runoff from the permafrost regions comprises direct runoff with a time lag of ~2 days, responding to rainfall. A comparison between the observed and calculated discharges shows that, in or around the smog-covered periods of 26 June to 1 July 2004 and 12–17 August 2005, the simulation significantly overestimated the discharge from the glacierized regions. The glacier-melt amount derived from the heat balance of Gulkana Glacier near site No. 8 during the smog-covered periods was comparable to that of the PDDA derived by equation (1) (personal communication, Mr Y. Narita, Hokkaido University). This suggests that there was englacial water storage in spite of large glacier-melt associated with high air temperatures (see T_{gl} in Fig. 3).

The simulated and observed suspended sediment concentration (SSC) series are shown in Fig. 7. The correlation between calculation and observation is very significant at r = 0.880 in 2002 (a = 96.4 and b = 2.3 in the $L \sim q$ equation), and at r = 0.922 in 2004 (a = 79.1 and b = 2.3), and also significant at r = 0.684 in 2005 (a = 88.4 and b = 2.3). The very high discharge and SSC from the glacierized regions in 2004 are due to the very high air temperatures. (Fig. 3). The relatively low correlation in 2005 results probably from the significant underestimation of discharge from glacierized regions in June and its overestimation in or after the smog-covered period

of 12–17 August 2005 (Fig. 6). It should be noted that the power b in the $L \sim q$

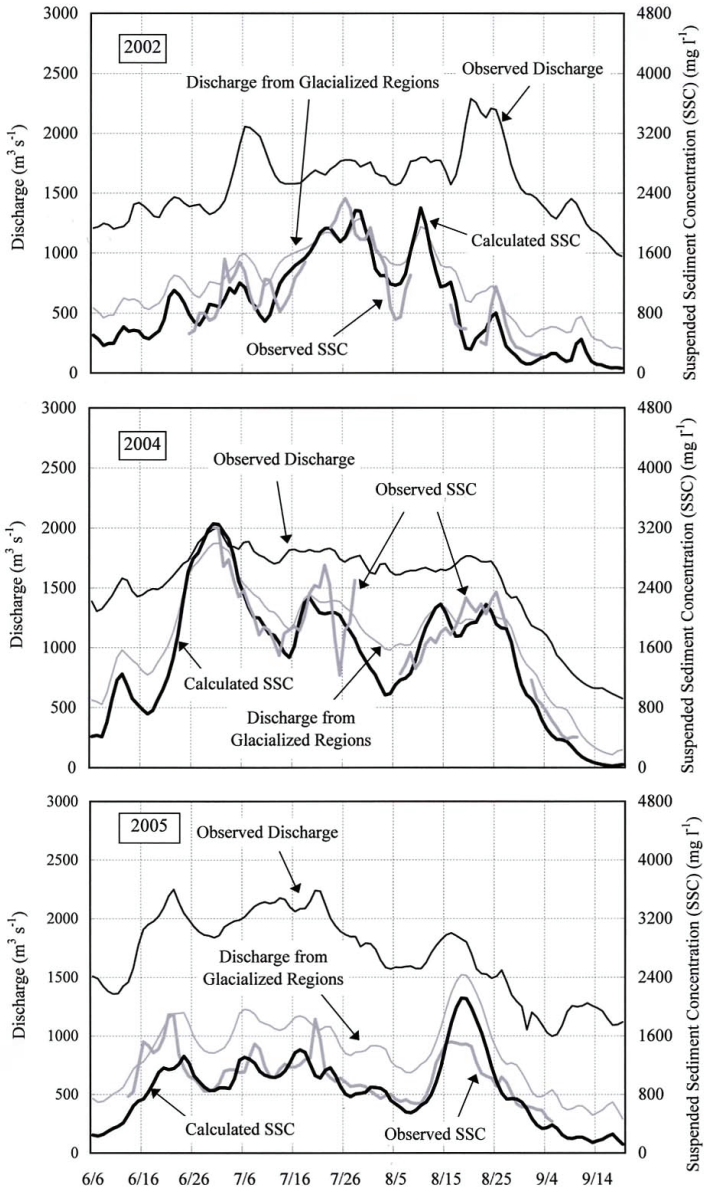

Fig. 7 Comparison between observed and simulated suspended sediment concentration (SSC) series. The observed and simulated discharge from the glacierized regions are also shown.

equation is constant at 2.3 and the coefficient a covers a relatively small range from 79.1 to 96.4. This suggests that the sediment erodibility is constant and the sediment availability for erosion is stable (Walling, 1974; Morgan, 1995; Asselman, 2000; Kido *et al*., 2007), probably because of the stable sediment supply at the base of the glacier.

The simulation results for SiO_2 are shown in Fig. 8. The best fit to the observed SiO_2 (r = 0.892) values was obtained by assigning a constant value of 244.3 μmol L^{-1} to the discharge from the bottom permafrost tank (i.e. base flow), and c = 0.0123 and d = 0.20 in the $L_{SI} \sim q$ equation. The dominant contribution of the base flow from permafrost regions suggests that the SiO_2 source is located mainly in the mineral layer

(Woo & Marsh, 2005). Increased direct runoff (discharge from the top and middle

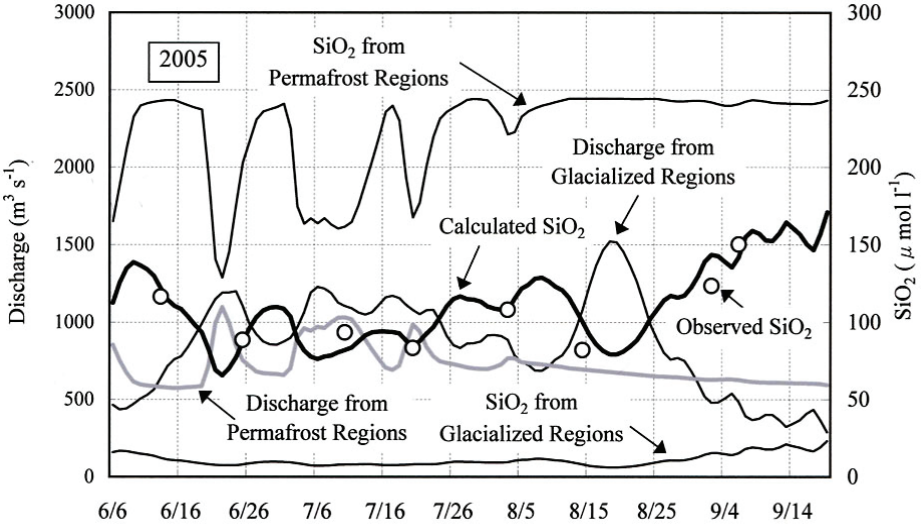

Fig. 8 Comparison between observed and simulated SiO_2 series. The simulated discharges from the glacierized and permafrost regions and their SiO_2 are also shown.

permafrost tanks) generated by rainfall tends greatly to decrease the SiO_2 concentration (Fig. 6).

CONCLUSIONS AND FUTURE WORK

Taking into account the effect of elevation on air temperature and rainfall, and using the accurate definition of glacierized area from a Landsat image, the runoff in the Tanana River, Alaska, was analysed using a tank model. Results revealed that, although the glacierized area occupied only 5.6% of the drainage area, the glacier-melt discharge accounted for 35.2%, 54.2% and 42.0% of the calculated total discharge in 2002, 2004 and 2005, respectively. The discharge from the permafrost regions is characterized by direct runoff in quick response to rainfall. The reasonable simulation of the sediment concentration and SiO_2 time series suggests that the suspended sediment and SiO_2 originate mostly from subglacial tills in the glacierized regions, and mainly from the mineral layer in the permafrost regions. The smog from large forest fires can change the water and heat balances of glaciers by decreasing inputs of solar radiation. The discharge simulations suggested englacial water storage during the smog-covered periods, since the calculations overestimated the glacier-melt discharge. The heat and water balances over the glacierized and permafrost regions should be explored in more detail because increasing aridity with global warming and the resultant increase in the number and magnitude of forest fires are likely to be critical in Alaskan river basins.

Acknowledgements We wish to express our gratitude to Messrs Matt Schellekens, Dennis Trabant and Rod S. March, USGS, Fairbanks, and to Mr Matt Sweetsir,

President of Yutana Barge Lines, LLC, Nenana, for their great help in the field survey. We are indebted to the three agencies NOAA, USGS and WRCC for the welcome supply of data. We are very grateful to Prof. Shun-ichi Akasofu, Director of IARC (International Arctic Research Center), and Ms Yoriko Freed, staff of IARC, the University of Alaska at Fairbanks for their official support in our field survey. This study was financially supported by the Foundation of the Hokkaido River Disaster Prevention Research Center (Director, Dr K. Hoshi) and by the Japan Aerospace Exploration Agency (JAXA) as part of the IARC/JAXA Project (supervised by Dr S. Saitoh, Faculty of Fisheries Sciences, Hokkaido University).

REFERENCES

Asselman, H. E. M. (2000) Fitting and interpretation of sediment rating curves. *J. Hydrol.* **234**, 228–248.

Brabets, T. P., Wang, B. & Meade, R. (2000) Environmental and hydrologic overview of the Yukon River Basin, Alaska and Canada. *Water-Resources Investigations Report 99-4204, US Geological Survey*.

Braithwaite, R. J. (1995) Aerodynamic stability and turbulent heat flux over a melting ice surface, the Greenland ice sheet. *J. Glaciol.* **41**, 562–571.

Brown, J., Ferrians, O. J., Jr, Heginbottom, J. A. & Melnikov, E. S. (1997) Circum-arctic map of permafrost and ground ice conditions. *US Geol. Survey Circum-Pacific Map Series*, Map CP-45.

Burrows, R. L., Emmett, W. W. & Parks, B. (1981) Sediment transport in the Tanana River near Fairbanks, Alaska, 1977-79. *Water-Resources Investigations Report, no. 81-20, US Geol. Survey*

Chikita, K. A., Morita, T, Wada, T. & Kido, D. (2006) Discharge and sediment load from a subarctic river basin: Tanana River, Alaska. *J. Japan Assoc. Hydrol. Sci.* **36**, 59–69.

Dingman, S. L. (2002) *Physical Hydrology*, 2nd edn. Prentice-Hall, Englewood Cliffs, New Jersey, USA.

Ferrians, O. J., Jr (1965) Permafrost map of Alaska. *US Geol. Survey Miscellaneous Geologic Investigations Map* I-445, scale 1:2 500 000.

Hamon, R. W. (1963) Computation of direct runoff amounts from storm rainfall. In: *Surface Waters* (Proc. Symp. at IUGG Assembly at Berkeley), 52–62. IAHS Publ. 63, IAHS Press, Wallingford, UK.

Kato, T., Kuroda, H. & Nakasone, H. (2003) Application of water quality tank model classified by land use to nitrogen load reduction plans. *Trans. Japan Soc. Irrig. Drain. Reclam. Engng* **224**, 97–104.

Kido, D., Chikita, K. A. & Hirayama, K. (2007) Subglacial drainage system changes of the Gulkana Glacier, Alaska: discharge and sediment load observations and modelling. *Hydrol. Processes* **21**, 399–410.

March, R. S. (2000) Mass balance, meteorological, ice motion, surface altitude, runoff and ice thickness data at Gulkana Glacier, Alaska, 1995 balance year. *Water-Resources Investigations Report, No. 00-4074, US Geol. Survey*

Mizunuma, K. & Chiu, C.-L. (1985) Prediction of combined snowmelt and rainfall runoff. *J. Hydraul. Engng ASCE* **111**, 179–193.

Morgan, R. P. C. (1995) *Soil Erosion and Conservation*, 2nd edn. Longman, London, UK.

Motoyama, H., Kobayashi, D. & Kojima, K. (1983) Water balance at a small watershed during the snowmelt season. *Low Temperature Sci., ser. A* **42**, 135–146.

Osawa, K. & Sakai, K. (2002) Construction of the suspended sediment runoff model for rainfall-sediment runoff analysis. *Trans. Japan Soc. Irrig. Drain. Reclam. Engng* **208**, 165–172.

Sugawara M. (1972) *A Method for Runoff Analysis*. Kyoritsu Shuppan Press, Tokyo, Japan (in Japanese).

Sugawara, M., Watanabe, I., Ozaki, E. & Katsuyama, Y. (1983) Reference manual for the TANK model. Report of National Research Center for Disaster Prevention, Tokyo, Japan.

Walling, D. E. (1974) Suspended sediment and solute yields from a small catchment prior to urbanization. In: *Fluvial Processes in Instrumented Watersheds* (ed. by K. J. Gregory & D. E. Walling), 169–192. Special Publ. 6. Institute of British Geographers, London, UK.

Woo, M.-K. & Marsh, P. (2005) Snow, frozen soils and permafrost hydrology in Canada, 1999-2002. *Hydrol. Processes* **19**, 215–229.

Yue, S. & Hashino, M. (2000) Unit hydrographs to model quick and slow runoff components of streamflow. *J. Hydrol.* **227**, 195–206.